Time-dependent quantum transport: Direct analysis in the time domain

Yu Zhu, Joseph Maciejko, Tao Ji, and Hong Guo
Center for the Physics of Materials and Department of Physics, McGill University, Montreal, QC H3A 2T8, Canada

Jian Wang
Department of Physics, The University of Hong Kong, Pokfulam Road, Hong Kong, China
(Received 30 September 2004; published 22 February 2005)

We present a numerical approach for solving time-dependent quantum transport problems in molecular electronics. By directly solving Green's functions in the time domain, this approach does not rely on the wide-band limit approximation thereby is capable of taking into account the detailed electronic structures of the device leads which is important for molecular electronics. Using this approach we investigate two typical situations: current driven by a bias voltage pulse and by a periodic field, illustrating that the computational requirement is no more than an inversion of a relatively small triangular matrix plus several matrix multiplications. We then present numerical results of time-dependent charge current for a one-dimensional atomic chain. The numerical solution recovers known results in the wide-band limit, and reveals physical behavior for leads with finite bandwidth.

DOI: 10.1103/PhysRevB.71.075317 PACS number(s): 73.63.Nm, 72.10.Bg, 72.30.+q, 73.40.Gk

I. INTRODUCTION

The idea of using single molecules as basic functional units for electronic device operation dates back to 1974 when Aviram and Ratner discussed the working principle of a molecular rectifier.[1] Since then there have been numerous theoretical and experimental investigations on charge and spin transport through various molecular systems in the metal-molecule-metal (MMM) configurations.[2] Here, the "molecule" indicates the device scattering region,[3–6] and the metal serves as device leads which extend to electron reservoirs far away where external voltage bias is applied so that a current is driven through. Since the ultimate goal of molecular electronics is in the application domain of nanotechnology, one of the most important questions which has yet to be answered, is how fast or how slow can a device turn on/off a current? In other words, if one applies a square voltage pulse of time duration τ, what is the time-dependent current $I(t)$ of the MMM system? What is $I(t)$ for other shapes of the time-dependent voltage? These questions should be answered before one can attempt to judge if a particular switching device is technologically viable. Indeed, some recent experimental efforts have already been devoted to the study of how does a molecular device respond to a gigahertz to even terahertz ac signals.[7,8] High frequency quantum transport in coherent conductors is also interesting in its own right. Upon applying an external field $\Delta(x,t)$ to a quantum conductor at position x and time t, wave functions of charge carriers acquire a phase factor $\exp[-i\int^t \Delta(x,t')dt']$, so that the spatial and temporal variables combine to play important roles in the time-dependent transport. For this reason ac quantum transport has rich behavior but its theory is complicated even for simple model analysis[9,10] without including any chemical detail present in a molecular device.

To make quantitative analysis of molecular devices in the form of MMM which typically involves large number of electrons, a practical and state-of-art dc transport formalism exists[11–13] which is based on carrying out the density functional theory (DFT) within the nonequilibrium Green functions (NEGF). Here the DFT takes care of atomic and chemical details of the device while the NEGF deals with the transport boundary conditions and nonequilibrium density matrix.[11–13] Quantitatively accurate comparisons to experimental data have been made using such a tool.[14,15] Despite its success in analyzing dc quantum transport, existing NEGF-DFT packages[11–13] cannot be directly applied to ac situations.

In principle, an ac theory could be based on self-consistent solutions of the time-dependent Kohn-Sham equation plus time-dependent electrodynamics. This is, however, impractical at the present stage due to its complexity and its prohibitively large computational demand. A simpler approach is to note the fact that an externally applied electric field, in most practical situations, is orders of magnitude smaller than the electrostatic field inside a molecule. Hence, one may start from a steady-state Hamiltonian, add the time-dependent field to the metal leads adiabatically, and then evaluate transport current. This idea has been widely adopted in mesoscopic physics and an elegant theory has been developed 10 years ago.[16] However, applications of this theory[17] rely on the so called wide-band limit (WBL)—an approximation in which device leads are assumed to have no energy dependent features. For molecular devices, however, the validity of the WBL is unclear because such devices are very sensitive to the molecule-metal contacts, hence, any approximation on the contact property should be carefully examined. In particular, recent interest in molecular devices sandwiched between semiconductors[18,19] requires careful examination on the effect of the nontrivial band structure of the leads, hence, quantitative predictions become difficult if the WBL is adopted. Therefore, it is highly desirable to develop an approach to calculate time-dependent quantum transport in MMM devices that does not rely on the WBL. Such an approach will then allow the time-dependent transport theory to

cooperate with the NEGF-DFT model[11,12] or a tight-binding model to account for atomic details.

It is the purpose of this paper to report a numerical approach to solve time-dependent quantum transport problems without the WBL approximation. We have found that for several very relevant time-dependent problems, Green's functions can be solved directly in the time domain without using the WBL. The method is applied to investigate time-dependent current driven by a bias voltage pulse and a periodic field. We compare results in the WBL and beyond the WBL, and demonstrate that the WBL approximation can lead to qualitatively different transport features.

The paper is organized as follows. In the next section, we briefly review the the NEGF formalism for time-dependent quantum transport.[17] To apply the formalism beyond the WBL, a possible approach is to work in the time domain and such a theory is presented in Sec. III. We confirm the theory and its associated numerics using an exactly solvable model. In Sec. IV, we investigate two important cases: time-dependent current driven by a voltage pulse and by a periodic field. As a demonstration, we apply our approach to a simple but nontrivial tight binding model of a one-dimensional atomic chain, which recovers known results in the WBL but reveals physical behavior beyond the WBL. Finally, a short summary is given in Sec. V.

II. NEGF THEORY FOR TIME-DEPENDENT TRANSPORT

We describe a MMM device by the following model Hamiltonian:

$$H = H_0 + H_{ext}(t), \tag{1}$$

where H_0 is the equilibrium or steady-state Hamiltonian of the device while $H_{ext}(t)$ is an externally applied time-dependent perturbation. In general H_0 has the following form:

$$H_0 = \sum_\beta H_\beta + H_C + H_T. \tag{2}$$

Here, H_β is the equilibrium Hamiltonian of the βth lead

$$H_\beta = \sum_k \epsilon_{\beta k} a^\dagger_{\beta k} a_{\beta k}, \tag{3}$$

where $a^\dagger_{\beta k}/a_{\beta k}$ creates/annihilates an electron in lead β with quantum number k. The second term H_C is the Hamiltonian of the device scattering region

$$H_C = \sum_n (\epsilon_n + U_n) c^\dagger_n c_n,$$

where $c^\dagger_n/c_n$ creates/annihilates an electron in the device scattering region at quantum state n, U_n is the single-particle potential energy. The third term H_T is the Hamiltonian describing the coupling between the device and the leads

$$H_T = \sum_{\beta k n} [v_{\beta k n} a^\dagger_{\beta k} c_n + \text{H.c.}],$$

where $v_{\beta k n}$ gives the coupling strength. In H_0, the electron-electron interactions are treated at the mean-field level so that only *quadratic* terms of creation/annihilation operations appear.

When there is no explicit time dependence in the Hamiltonian, i.e., $H_{ext}(t)=0$, the steady-state quantum transport problem is determined by H_0, and can be solved for molecular devices in the MMM configuration. Such a steady-state analysis involves a self-consistent calculation of device Hamiltonian H_0 by the density functional theory combined with nonequilibrium Green's functions in the energy space, as shown in Refs. 11 and 12. From now on, we will assume that H_0 has been calculated this way or known from some tight binding parametrization, and focus on how to solve the problem when $H_{ext}(t) \neq 0$. To proceed, we further assume that the time-dependent perturbation $H_{ext}(t)$ is locally *uniform* on each lead, and the energy levels in the lead are shifted adiabatically with it. $H_{ext}(t)$ has the form

$$H_{ext}(t) = \sum_k \Delta_\beta(t) a^\dagger_{\beta k} a_{\beta k},$$

where $\Delta_\beta(t)$ is the time-dependent perturbation field. For the following analysis, it is convenient to absorb $\Delta_\beta(t)$ into a phase factor by applying an unitary transformation discussed in Ref. 20 so that the coefficient $v_{\beta k n}$ becomes

$$v_{\beta k n}(t) = v_{\beta k n} \exp\left[-i \int^t dt' \Delta_\beta(t') \right]. \tag{4}$$

For the time-dependent problem of Hamiltonian (1), a general formulation for quantum transport based on the NEGF technique has been established before.[16] An extension of this theory to include displacement current was addressed in Ref. 10. It has been shown that the current in a lead labeled with β at time t can be written in terms of Green's function and self-energy[16]

$$I_\beta(t) = \frac{2e}{\hbar} 2\ \text{Re} Tr \int dt_1 [G^r(t,t_1)\Sigma^<_\beta(t_1,t) + G^<(t,t_1)\Sigma^a_\beta(t_1,t)], \tag{5}$$

where G is the Green's function matrix of the scattering region defined by $G_{mn}(t_1,t_2) \equiv \langle\langle c_m(t_1) | c^\dagger_n(t_2)\rangle\rangle$; Σ_β is the self-energy matrix due to coupling between the scattering region and the leads, defined by $\Sigma_{\beta,mn}(t_1,t_2) \equiv \Sigma_k v^*_{\beta k m}(t_1) \times \langle\langle a_{\beta m}(t_1) | a^\dagger_{\beta n}(t_2)\rangle\rangle v_{\beta k n}(t_2)$. (The notation $\langle\langle A(t_1)|B(t_2)\rangle\rangle$ is used to represent all of the real time Green's functions such as retarded Green function $\langle\langle A(t_1)|B(t_2)\rangle\rangle^r \equiv -i\theta(t_1-t_2) \times \langle\{A(t_1),B(t_2)\}\rangle$, lesser Green function $\langle\langle A(t_1)|B(t_2)\rangle\rangle^< \equiv i\langle B(t_2)A(t_1)\rangle$, etc.); and the trace is over the degree of freedom in the scattering region. G^r and $G^<$ satisfy the Dyson equation and Keldysh equation, respectively,

$$G^r(t_1,t_2) = g^r(t_1,t_2) + \int\int dt_3 dt_4 g^r(t_1,t_3)\Sigma^r(t_3,t_4)G^r(t_4,t_2), \tag{6}$$

$$G^<(t_1,t_2) = \int\int dt_3 dt_4 G^r(t_1,t_3)\Sigma^<(t_3,t_4)G^a(t_4,t_2). \quad (7)$$

The total self-energy Σ is a summation over contributions from self-energy of each lead, which can be expressed as[20]

$$\Sigma_\beta^{r,<}(t_1,t_2) = \int \frac{d\epsilon}{2\pi} e^{-i\epsilon(t_1-t_2)} \tilde{\Sigma}_\beta^{r,<}(\epsilon) \exp\left[-i\int_{t_2}^{t_1} \Delta_\beta(t)dt\right],$$

where $\tilde{\Sigma}_\beta^{r,<}(\epsilon)$ is the Fourier transform of the self-energy in the absence of any time-dependent perturbation.

In order to calculate the transport current from Eq. (5), one needs to solve the integral Eq. (6) and then evaluate the multiple integrals in Eq. (7). Since these are difficult to do, in practice one usually applies an additional approximation, the so called wide-band limit.[21–23] In the WBL, $\tilde{\Sigma}_\beta^r(\epsilon)$ is assumed to be an energy-independent constant so that $\Sigma_\beta^r(t_1,t_2)$ is proportional to $\delta(t_1-t_2)$. Consequently, $G^r(t_1,t_2)$ becomes exactly the same as that without the time-dependent perturbation, and the current formula (5) only contains $G^<(t,t)$ for which the double integral in Eq. (7) can be reduced to two single integrals. This procedure drastically simplifies subsequent analysis. The WBL is reasonable if the leads have no energetic features near its Fermi energy. But it fails to describe leads with a finite bandwidth and the energy dependence of the leads' density of states (DOS). These situations are important for molecular electronics because the detailed chemistry in molecule-lead contact region can dominate the entire transport features. In the next section, we shall develop a numerical approach for solving Eqs. (5)–(7) beyond the WBL.

III. TIME DOMAIN DECOMPOSITION

One always has the freedom to choose working either in the real space or in the Fourier-transformed space. Most of the time, Fourier transform can help to convert differential or integral equations into algebraic equations, which greatly simplifies the mathematical procedure. The time-dependent transport problem defined in Eqs. (5)–(7), however, is an exception because in the presence of time-dependent perturbation, the Green's function $G(t_1,t_2)$ is neither a function of t_1-t_2 nor is subjected to periodic boundary condition for each time variable. Even in the presence of periodic field with period T, the Green function satisfies $G(t_1+T,t_2+T) = G(t_1,t_2)$ rather than $G(t_1+T,t_2) = G(t_1,t_2)$ and $G(t_1,t_2+T) = G(t_1,t_2)$. While one can use a double Fourier transform to convert Green's functions into energy space,[24,25] in general this does not simplify matters without further approximations.

Alternatively, let us work *directly* in the time domain by discretizing the time variables in Eqs. (5)–(7). In the time domain, the Green's functions become matrices; the integral Eq. (6) becomes a matrix equation; the multiple integrals in Eqs. (6) and (7) become matrix multiplication; and more importantly, the temporal features of the Green's functions are exposed explicitly in the structure of matrices. A naive computation based on this idea, however, does not work because the integral variables in Eqs. (5)–(7) run from $-\infty \to +\infty$ so that one needs to deal with huge (if not infinitely large) matrices: in particular one must invert such a huge matrix to solve Eq. (6) that is a computational challenge. Fortunately, we found that for quantum transport problems in an open system, the time limits $-\infty \to +\infty$ in Eqs. (5)–(7) can be effectively truncated to a finite time domain having a scale of the correlation time [see Eq. (8) below]. For some typical cases the finite time domain can be further decomposed into smaller blocks: the Green's function in Eq. (6) for each block can be calculated efficiently without needing to invert any huge matrix (see next section for detailed discussion). We call this technique "time domain decomposition" (TDD).

TDD is based on physically motivated grounds. First, the time $=+\infty$ limit in Eqs. (5)–(7) can be replaced by the upper time limit concerned in the calculation (not an approximation), as the "future" must not affect what happens "now." Second, the time $=-\infty$ limit can be *cutoff* at some remote past whose phase memory is totally lost by now (a well-controlled approximation). In an isolated system, such correlation can be infinite long: the initial state at $t=-\infty$ can determine the present state by the Schrödinger equation. But for an open system such as a MMM device, the lifetime of quantum scattering states in the device scattering region is finite, hence, a finite characteristic correlation time exists in this problem. Mathematically, Green's functions for a transport problem scale as $e^{-\Gamma|t_1-t_2|}$ at large time, where Γ is the total coupling strength of the device scattering region to its environment. This gives a natural cutoff in time

$$T_C = \frac{\hbar}{\Gamma}. \quad (8)$$

One may, therefore, *practically* take $G^{r,a,<}(t_1,t_2) \approx 0$ if $|t_1 - t_2| > T_C$. With this lower time cutoff, Eqs. (5)–(7) can be calculated directly in the time domain.

To show that TDD is quantitatively accurate, we present an exactly solvable transport problem and compare the numerical results obtained in TDD with that of the analytical solution. The problem is described as follows: consider a device whose scattering region consists of a single energy level, and the device is coupled to a single lead with *finite band width W* (Lorentzian shape). The retarded self-energy can be obtained as

$$\Sigma^r(\epsilon) = \Gamma \int \frac{d\epsilon_k}{2\pi} \frac{1}{\epsilon - \epsilon_k + i0^+} \frac{W^2}{W^2+\epsilon_k^2} = \frac{\Gamma}{2}\frac{W}{\epsilon + iW}. \quad (9)$$

At the time $t=0$, the energy level abruptly jumps from E_1 to E_2 due to some external perturbation.

For this simple problem, the retarded Green's function can be derived analytically (see the Appendix for more details):

$$G^r(t_1>0,t_2>0) = -i\theta(t_1-t_2)h(t_1-t_2,E_1), \quad (10)$$

$$G^r(t_1<0,t_2<0) = -i\theta(t_1-t_2)h(t_1-t_2,E_2), \quad (11)$$

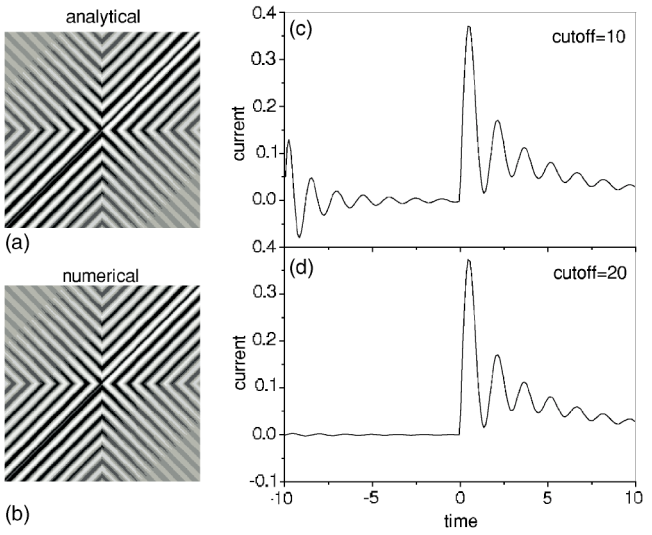

FIG. 1. Solution of an exactly solvable problem. (a) and (b) are the gray-scale plot of the Green's function matrix $G^r(t_1,t_2)$ obtained from the exact analytical solution and the numerical solution using TDD, respectively. Notice that the G^r matrix is zero in the upper triangle. We plot the real part of matrix elements in the upper triangle and the imaginary part in the lower triangle. (c) and (d) are numerical results of $I(t)$ curves with different lower time cutoffs in TDD: (c) is for a small cutoff such that $I(t)$ deviates from the exact result when time is near the lower cutoff; (d) is for larger cutoff which is indistinguishable from the exact result (because they are indistinguishable, the exact result is not shown). We set $\hbar=e=1$. Other parameters are: $E_1=4$, $E_2=-4$, $\Gamma=1$, $W=2$.

$$G^r(t_1>0,t_2<0) = -i[h(t_1,E_2)h(-t_2,E_1) + f(t_1,E_2)f(-t_2,E_1)], \tag{12}$$

$$G^r(t_1<0,t_2>0) = 0, \tag{13}$$

in which

$$h(t,E_l) \equiv \frac{E_l^+ + iW}{E_l^+ - E_l^-} e^{-iE_l^+ t} + \frac{E_l^- + iW}{E_l^- - E_l^+} e^{-iE_l^- t},$$

$$f(t,E_l) \equiv \frac{\sqrt{\Gamma W/2}}{E_l^+ - E_l^-}(e^{-iE_l^+ t} - e^{-iE_l^- t}),$$

$$E_l^\pm \equiv \tfrac{1}{2}[E_l - iW \pm \sqrt{E_l^2 + 2iWE_l - W^2 + 2\Gamma W}].$$

In the last expression, $E_l^\pm$ correspond to the $+/-$ signs on the right-hand side. Figure 1(a) shows a gray-scale plot of the retarded Green's function of this exact solution. Then we solve the same problem by numerically computing $G^r(t_1,t_2)$ matrix using the TDD technique (200 time points are used in the computation). The result is shown in Fig. 1(b), which is indistinguishable from the exact solution in Fig. 1(a). Figures 1(c) and 1(d) show time-dependent current $I(t)$ versus time t obtained from TDD for two different cutoffs. For a small cutoff [Fig. 1(c)], the result deviates significantly from the exact solution when t approaches the lower cutoff, although the result is still reliable when t is far from the lower cutoff. For larger cutoff [Fig. 1(d)], the numerical $I(t)$ is essentially identical to the exact solution in the full time range. We conclude that to obtain a correct current behavior at some time t_0, one needs to compute the Green's function down to time t_0-T_C, as the quantum system cares about the history at time scale T_C.

Basically, there are two approximations in the TDD technique, one is the discretization in time, the other is the lower cutoff in time. The validity of the first approximation requires that the time interval used in the discretization is smaller than the characteristic scale of the variation in Green's functions. This scale corresponds to $\hbar$ over the maximum energy scale in the problem, e.g., the coupling strength Γ, the peak value of the bias pulse Δ, etc. The second approximation relies on the physics discussed in the last paragraph, i.e., there exists a characteristic correlation time in an open quantum system beyond which two physical events are uncorrelated. The calculation of G^r is more accurate than $G^<$, in the sense that G^r only involves the first approximation while $G^<$ relies on both. This is because the time variables of retarded quantities in the Dyson equation are constrained by time sequence (see next section for details). While there is no constraint for lesser quantities, one must make a truncation to obtain a finite matrix. We emphasize that both approximations are well controlled. In practice, one may estimate the correlation time and discretization interval by relevant energy scales, and check the validity of the two approximations by doubling or halving these values in a numerical computation until the results have no significant change.

Direct inversion of Green's function matrix with the time scale T_C is able to deal with *arbitrary* time-dependent perturbations. But a serious numerical problem will arise when the coupling strength $\Gamma \to 0$ so that the cutoff $T_C \to \infty$, where one encounters a huge matrix inversion in TDD. This situation occurs when the device scattering region is weakly coupled to the leads. However, we found that by taking advantage of *specific* properties of time-dependent perturbation, large T_C limit can also be efficiently treated in the TDD. These special cases cover a wide range of physically important situations, such as sending a pulsed signal or applying a periodic field to the MMM device, as demonstrated in the next section.

IV. CURRENT DRIVEN BY VOLTAGE PULSE AND PERIODIC FIELD

In this section, we investigate two most relevant cases: electric current driven by a bias voltage pulse and by a periodic field. We show that the specific features of the time-dependent perturbation will greatly simplify the computation in TDD, so that calculation for large T_C limit is possible with relatively small computational demand.

Since the equilibrium or steady-state Hamiltonian H_0 can be computed by applying the NEGF-DFT *ab initio* method of Refs. 11 and 26, or by assuming a simple tight binding form,[27] let us assume that the equilibrium or steady-state Green's function of the scattering region $\tilde{G}^r$ and the self-energy $\tilde{\Sigma}^r$ of the leads are known from H_0. Upon applying a time-dependent signal $\Delta_\beta(t)$ to the βth lead, the total Hamil-

tonian has the form of Eq. (1). The retarded Green's function of the total Hamiltonian H satisfies a "modified" Dyson equation

$$G^r(t_1,t_2) = \tilde{G}^r(t_1,t_2) + \int\int dt_3 dt_4 \tilde{G}^r(t_1,t_3) V^r(t_3,t_4) G^r(t_4,t_2), \tag{14}$$

where V^r is a summation over V^r_β with

$$V^r_\beta(t_1,t_2) \equiv \tilde{\Sigma}^r_\beta(t_1-t_2)\left\{ \exp\left[-i\int_{t_2}^{t_1} \Delta_\beta(t)dt \right] - 1 \right\}. \tag{15}$$

This modified Dyson equation differs from the usual Dyson Eq. (6), using $\tilde{G}^r$ instead of g^r as its unperturbed Green's function. It means that the time-dependent calculation is built on the equilibrium or steady-state Green's functions.

A. Pulsed signal

A bias voltage pulse applied to βth lead can be considered to have the following form:

$$\Delta_\beta(t) = \begin{cases} 0 & \text{for } t<0 \text{ or } t>\tau_{pulse} \\ \neq 0 & \text{for } 0<t<\tau_{pulse} \end{cases}.$$

To simplify notation, hereafter we call $t<0$ the T_- region; $0<t<\tau_{pulse}$ the T_τ region; and $t>\tau_{pulse}$ the T_+ region.

To solve Eq. (14) with the TDD technique, there are two mathematical properties to rely on: (a) By definition, time variables in the retarded quantities like retarded Green's functions and retarded self-energies are sorted according to time sequence, e.g., $t_1>t_3>t_4>t_2$ in Eq. (14). This property is general for the retarded Dyson equation. (b) From Eq. (15), V^r_β has the property that $V^r_\beta(t_1,t_2)\equiv 0$ if t_1, $t_2 \in T_-$ or t_1, $t_2 \in T_+$. This property is specific for the pulsed signal. Accordingly, the retarded Green's function G^r in Eq. (14) can be subdivided into a 3×3 block matrix in the time domain

$$G^r(t_1,t_2) = \begin{array}{c|ccc} t_1 \backslash t_2 & - & \tau & + \\ - & G^r_{--} & 0 & 0 \\ \tau & G^r_{\tau-} & G^r_{\tau\tau} & 0 \\ + & G^r_{+-} & G^r_{+\tau} & G^r_{++} \end{array} \tag{16}$$

and the remaining task is to evaluate these blocks. The three zeros in the upper right triangle are due to the property (a).

Below we show that the computation of those nonzero blocks is equivalent to an inverse of a small matrix plus some matrix multiplications. First, let us consider the block G^r_{--} (or G^r_{++}), whose time variables t_1, t_2 belong to T_- (or T_+). Because of the property (a), those intermediate variables t_3, t_4 in Eq. (14) also belong to T_- (or T_+). Due to the property (b), $V^r(t_3,t_4)=0$, and therefore $G^r_{--}=\tilde{G}^r_{--}$ and $G^r_{++}=\tilde{G}^r_{++}$. Since $\tilde{G}$ is known already, these blocks do not need any new computation. Second, for the block $G^r_{\tau\tau}$, $t_1,t_2 \in T_\tau$ and therefore $t_3,t_4 \in T_\tau$, in Eq. (14). As a result, Eq. (14) becomes a *closed* equation for $G^r_{\tau\tau}$, which can be solved by matrix inversion. Third, consider the blocks $G^r_{+\tau}$ and $G^r_{\tau-}$. For block $G^r_{+\tau}$, the time variables $t_1 \in T_+$ and $t_2 \in T_\tau$. In Eq. (14), t_4 must belong to T_τ, otherwise either $t_4 \in T_-$ which contradicts to the time sequence $t_4>t_2$, or $t_4 \in T_+$ (hence, $t_3 \in T_+$ due to $t_3>t_4$) which leads to $V^r(t_3,t_4)=0$. Thus both time variables in $G^r(t_2,t_4)$ belong to T_τ, and the block $G^r_{+\tau}$ is related to the known block $G^r_{\tau\tau}$ by the Dyson equation. For the block $G^r_{\tau-}$, one can apply a similar argument to an alternative form of the Dyson equation

$$G^r(t_1,t_2) = \tilde{G}^r(t_1,t_2) + \int\int dt_3 dt_4 G^r(t_1,t_3) V^r(t_3,t_4) \tilde{G}^r(t_4,t_2), \tag{17}$$

and show that t_3 must belong to T_τ, and the block $G^r_{\tau-}$ is also related to $G^r_{\tau\tau}$ by this equation. Finally, consider the block G^r_{+-}. In the same way, one can apply the properties (a) and (b) to a more fancy form of the Dyson equation [easily to be verified by substituting Eq. (17) into Eq. (14)]:

$$\begin{aligned} G^r(t_1,t_2) = \tilde{G}^r(t_1,t_2) &+ \int\int dt_3 dt_6 \tilde{G}^r(t_1,t_3) V^r(t_3,t_6) \tilde{G}^r(t_6,t_2) \\ &+ \int\int\int\int dt_3 dt_4 dt_5 dt_6 \tilde{G}^r(t_1,t_3) V^r(t_3,t_4) G^r(t_4,t_5) \\ &\times V^r(t_5,t_6) \tilde{G}^r(t_6,t_2), \end{aligned}$$

and show that $t_4 \in T_\tau$ and $t_5 \in T_\tau$, therefore G^r_{+-} is related to $G^r_{\tau\tau}$ by this equation.

For a voltage pulse, the time duration $\tau_{pulse} \ll \hbar/\Gamma$, therefore $T_\tau \ll T_+$, T_-. The above scheme reduces the inversion of a huge matrix associated with the scale $T_+ + T_\tau + T_-$ to the inversion of a much smaller matrix associated with the scale T_τ. The inversion itself is also much simpler than inverting a general matrix because the retarded Green's function matrix in the time domain has nonzero elements only in the lower matrix triangle. In practice, one first generates V^r and $\tilde{G}^r$ matrices from the unperturbed Hamiltonian H_0, then derives $G^r_{\tau\tau}$ by matrix inversion, after that computes other nonzero blocks by matrix multiplications. For the other limit, the long pulse whose duration $\tau_{pulse} \gg \hbar/\Gamma$, one can simply divide the pulsed signal into several pieces each with length $\sim \hbar/\Gamma$, and deal with each piece using the TDD technique discussed in the last section.

The above discussion of solving the blocks in Eq. (16) is based on the integral Dyson equation and the specific property of the voltage pulse. If we look at the problem from a mathematical point of view, the reasoning becomes much more straightforward. Consider a general 3×3 block triangular matrix [e.g., Eq. (16)]:

$$A = \begin{pmatrix} A_{11} & 0 & 0 \\ A_{21} & A_{22} & 0 \\ A_{31} & A_{32} & A_{33} \end{pmatrix}, \tag{18}$$

whose inversion must also be a 3×3 block triangular matrix

$$B=\begin{pmatrix} B_{11} & 0 & 0 \\ B_{21} & B_{22} & 0 \\ B_{31} & B_{32} & B_{33} \end{pmatrix}.$$

Hence $AB=I$ implies $B_{11}=A_{11}^{-1}$, $B_{22}=A_{22}^{-1}$, $B_{33}=A_{33}^{-1}$, $B_{21}=-B_{11}A_{21}B_{11}$, $B_{32}=-B_{33}A_{32}B_{22}$, and $B_{31}=-B_{33}A_{31}B_{11}+B_{33}A_{32}B_{22}A_{21}B_{11}$. Notice that only three matrix inversions appear in the expressions of B blocks (B_{11}, B_{22}, and B_{33}), while other blocks are obtained by multiplications of known matrices. Now, recall that the solution of the Dyson equation can be expressed as $G^r=(I-\tilde{G}^r\Sigma^r)^{-1}\tilde{G}^r$, solving integral Eq. (14) is therefore equivalent to inverting a huge matrix ($I-\tilde{G}^r\Sigma^r$) followed by a matrix multiplication in the time domain. Specially in the pulse case, the huge matrix can be subdivided into a 3×3 block matrix and $\Sigma_{11}^r=\Sigma_{33}^r=0$ due to the property (b) discussed above. Hence, the inversions of B_{11} and B_{33} lead to nothing but the equilibrium or steady-state Green's function which is already known; only one inversion is necessary to derive B_{22}. With this mathematical argument, identifying the corresponding matrix blocks between Eq. (16) and Eq. (18), it is not surprising to find the same result for the blocks in (16), in matrix form: (i) $G_{--}^r=\tilde{G}_{--}^r$ and $G_{++}^r=\tilde{G}_{++}^r$. (ii) $G_{\tau\tau}^r$ satisfies $G_{\tau\tau}^r=\tilde{G}_{\tau\tau}^r+\tilde{G}_{\tau\tau}^r V_{\tau\tau}^r G_{\tau\tau}^r$, which can be solved by direct matrix inversion. (iii) $G_{\tau-}^r$ and $G_{+\tau}^r$ can be related to $G_{\tau\tau}^r$ by $G_{\tau-}^r=\tilde{G}_{\tau-}^r+\Sigma_s\, G_{\tau\tau}^r V_{\tau s}^r \tilde{G}_{s-}^r$ and $G_{+\tau}^r=\tilde{G}_{+\tau}^r+\Sigma_s\, \tilde{G}_{+s}^r V_{s\tau}^r G_{\tau\tau}^r$, respectively. (iv) G_{+-}^r can be related to $G_{\tau\tau}^r$ by $G_{+-}^r=\tilde{G}_{+-}^r+\Sigma_{s,t}\, \tilde{G}_{+s}^r V_{st}^r \tilde{G}_{t-}^r+\Sigma_{s,t}\, \tilde{G}_{+s}^r V_{s\tau}^r G_{\tau\tau}^r V_{\pi}^r \tilde{G}_{t-}^r$. Finally, we point out that this numerical method to deal with the pulse signal can be easily generalized to investigate the transition between two steady states, i.e., the current flow driven by a step-like bias profile (see also the Appendix).

B. Periodic field

For a periodic field, $\Delta_\beta(t+T)=\Delta_\beta(t)$ where T is the period. Here we will not repeat the complicated analysis on the integral Dyson equation. Instead, let us look at the Green's function matrix in the time domain where the characteristics of time dependence is clearly exposed. It is straightforward to observe that in the presence of a periodic field, the Green's functions have the property $G(t_1+T,t_2+T)=G(t_1,t_2)$. In the time domain, the retarded quantities such as $\tilde{G}^r$, V^r, and G^r share the same matrix structure

$$\begin{array}{cccccc} t_1\backslash t_2 & T & 2T & 3T & 4T & \cdots \\ T & A_0 & 0 & 0 & 0 & \cdots \\ 2T & A_1 & A_0 & 0 & 0 & \cdots \\ 3T & A_2 & A_1 & A_0 & 0 & \cdots \\ 4T & A_3 & A_2 & A_1 & A_0 & \cdots \\ \cdots & \cdots & \cdots & \cdots & \cdots & \cdots \end{array}. \tag{19}$$

We name the ensemble of matrices with the structure (19) as "T-class." It turns out that solving the Dyson equation in the presence of periodic field is equivalent to invert a T-class matrix plus a T-class matrix multiplication. It is easy to see that the product of two T-class matrices is still a T-class matrix. Explicitly, let $C=AB$ where A and B are T-class matrices, C is also a T-class matrix with $C_k=\Sigma_{i=0}^k A_i B_{k-i}$. The inversion of a T-class matrix is still a T-class matrix. Explicitly, let $B=A^{-1}$ where A is a T-class matrix, B is also a T-class matrix with $B_0=A_0^{-1}$ and $B_k=-B_0\Sigma_{i=0}^{k-1}A_{k-1}B_i$ for $k\geqslant1$. Again, we see that the scale of the matrix needs to be inverted is no more than T rather than the cutoff $\hbar/\Gamma$. In practice, if $\hbar/\Gamma<T$, one solves the Dyson equation directly by matrix inversion. On the other hand, if $\hbar/\Gamma>T$, one first derives G_0^r (the A_0 block) by matrix inversion, then computes $G_n^r(n\geqslant1)$ blocks by matrix multiplication until $nT>\hbar/\Gamma$.

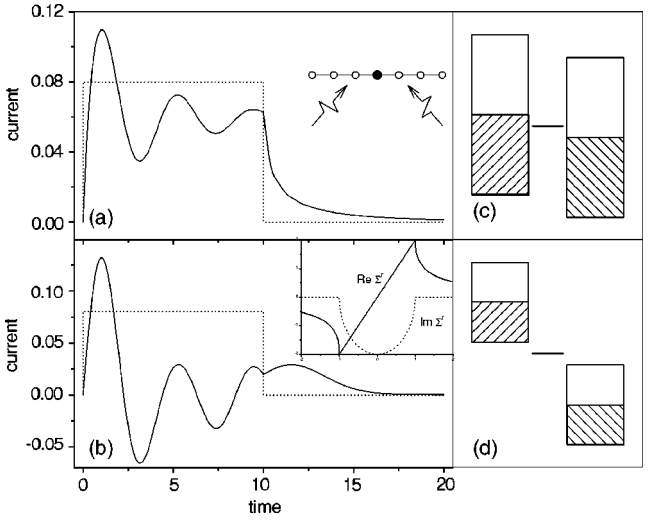

FIG. 2. $I(t)$ curves (solid line) of the 1D atomic chain in response to a rectangular bias voltage pulse (dotted line). The pulse has an amplitude $\Delta_L=-\Delta_R=1.5$ and duration $\tau_{pulse}=10$. (a) is obtained using the WBL with parameters $v_0=4$, $v_L=v_R=0.5$, due to which the bandwidth is $W=16$ and the coupling strength is $\Gamma_0=0.25$. (b) is obtained with TDD for a finite bandwidth, with parameters $v_0=0.5$, $v_L=v_R=0.25$ and, hence, $W=2$ and $\Gamma_0=0.5$. The inset of (a) schematically shows the 1D atomic chain under consideration; the inset of (b) plots the real and imaginary part of the retarded self-energy. (c) and (d) illustrate the energy diagrams in case of WBL and finite bandwidth, respectively.

C. Numerical example: One-dimensional atomic chain

We now apply the TDD Eqs. (16) and (19) to investigate a simple one-dimensional (1D) tight binding model of an infinitely long chain of atoms, shown in the inset of Fig. 2(a). In this chain, one atom has a different energy level than the rest, and this atom provides the scattering region, the entire system mimics an open structure in the MMM configuration. The Hamiltonian of the chain, Eq. (2), is specified as follows:

$$H_0 = \sum_{\beta=L,R} H_\beta + H_C + H_T,$$

$$H_\beta = \sum_{<ij>} v_0 a_{\beta i}^\dagger a_{\beta j} + \text{H.c.},$$

$$H_C = E_0 c^\dagger c,$$

$$H_T = \sum_{\beta=L,R} v_\beta(t) a_{\beta 0}^\dagger c + \text{H.c.}, \tag{20}$$

where $\langle ij \rangle$ refer to the index pair of adjacent neighbors in the 1D chain, $a_{\beta 0}^\dagger$ is the creation operator for the outmost site of βth lead toward the central atom, and the time-dependent field has been transformed to the hopping parameter [see Eq. (4)]:

$$v_\beta(t) = v_\beta \exp\left[-i \int^t dt' \Delta_\beta(t') \right].$$

Here H_β is nondiagonal which differs from Eq. (3). Although the difference can be formally eliminated by diagonalization, it is more convenient to work with this nondiagonal form so that one can use the surface Green's function technique to construct self-energy for the semi-infinite lead.[11,12]

Due to the simplicity of the model, the equilibrium self-energy of the lead to the scattering region can be obtained analytically[28]

$$\tilde{\Sigma}_\beta^r(\epsilon) = \begin{cases} \dfrac{2v_\beta^2}{\epsilon + i\sqrt{4v_0^2 - \epsilon^2}} & |\epsilon| < 2v_0 \\ \dfrac{2v_\beta^2}{\epsilon + sgn(\epsilon)\sqrt{\epsilon^2 - 4v_0^2}} & |\epsilon| > 2v_0 \end{cases},$$

where ϵ is the electron energy. Clearly, this self-energy is beyond the wide-band limit and we plot it in Fig. 2(b): the imaginary part of $\tilde{\Sigma}_\beta^r(\epsilon)$ indicates a finite bandwidth $4v_0$. The effective total coupling strength can be estimated as $\Gamma_0 = 4v_\beta^2/v_0$. We Fourier transform $\tilde{\Sigma}_\beta^r(\epsilon)$ back to time which can be analytically accomplished

$$\tilde{\Sigma}_\beta^r(t_1 - t_2) = -i\theta(t_1 - t_2)\frac{v_1^2}{v_0(t_1 - t_2)} J_1[2v_0(t_1 - t_2)],$$

$$\tilde{\Sigma}_\beta^<(t_1 - t_2) = i\frac{v_1^2}{2v_0(t_1 - t_2)}\{J_1[2v_0(t_1 - t_2)] + iH_1[2v_0(t_1 - t_2)]\},$$

where $J_n(z)$ is the nth order Bessel function and $H_n(z)$ the nth order Struve-H function.

By numerically evaluating Eqs. (16) and (19), we investigate the time-dependent current $I(t)$ in the atomic chain driven by a rectangular pulse and by a sinusoidal signal, results are shown in Figs. 2 and 3, respectively $[I_L(t) = -I_R(t) \equiv I(t)]$. In Figs. 2(a) and 3(a), the parameters are chosen such that the bandwidth of the leads is much larger than all other energy scales, and the resulting $I(t)$ curves recover those obtained within the WBL approximation.[17]

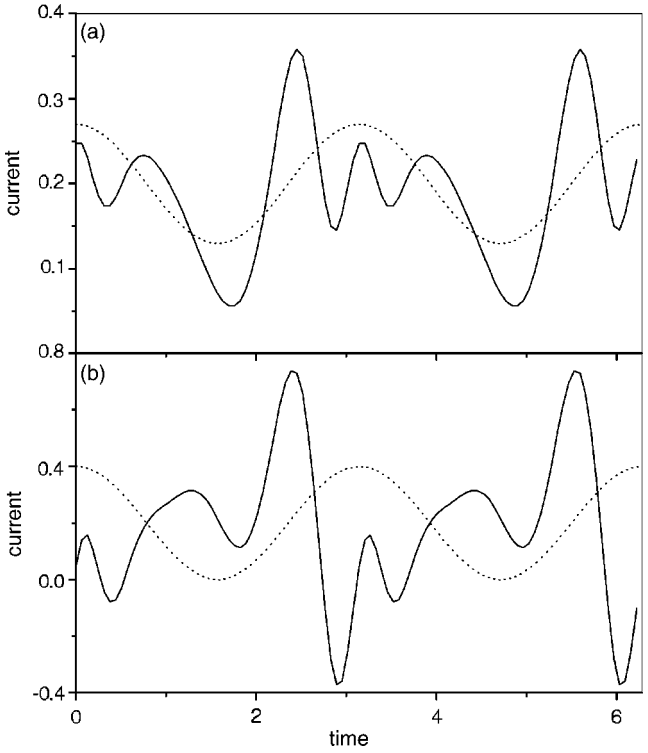

FIG. 3. $I(t)$ curves (solid line) of the 1D atomic chain in response to a sinusoidal bias signal (dotted line). The ac signal has amplitude $\Delta_L = -\Delta_R = 5$ and frequency $\omega = 2$, imposed on a dc voltage $V_L = -V_R = 5$. (a) is obtained using the WBL, with parameters $v_0 = 9$, $v_L = v_R = 1.5$, due to which the bandwidth is $W = 36$ and the coupling strength is $\Gamma_0 = 1$. (b) is obtained using TDD for the case of finite bandwidth, with parameters $v_0 = 2.5$, $v_L = v_R = 1.5$, due to which $W = 10$ and $\Gamma_0 = 3.6$.

Figures 2(b) and 3(b), in contrast, correspond to the case of finite bandwidth, and the behavior of $I(t)$ curves is *qualitatively* different from the WBL result.

In Fig. 2(b), we set the amplitude of the rectangular pulse larger than the bandwidth of the leads. It is interesting to observe that the current can be temporarily driven to *negative* values even though the bias pulse is strictly positive. This is a direct consequence of a finite bandwidth. For leads in the wide-band limit, the current is always positive and exhibits damping oscillation around its steady state value. On the other hand, in the zero-band limit the system reduces to three quantum levels and a perturbation on these levels will stimulate sinusoidal oscillation of charges among them. Finally, in the case of a finite bandwidth, the current behavior is between these two limit situations: we now have a damping oscillation around zero. The reason for a zero steady-state current is because of the fact that energy bands of the left and right leads are shifted to opposite directions: when there is no overlap between them, current cannot flow since no states are available in the leads [see Fig. 2(d), and compare Fig. 2(d) with the WBL band diagram of Fig. 2(c)]. We believe this effect can be exploited to measure the bandwidth of leads by tuning the amplitude of the voltage pulse.

In Fig. 3(b), current is driven by a sinusoidal voltage signal imposed on a dc bias. Similar to the case of pulsed signal, the $I(t)$ curve behaves qualitatively different from that of

the WBL: the current does not reach its minimum at the voltage minimum, and the current is driven to *negative* at the voltage maximum. The behavior can be, roughly, understood in an analogous way as to Fig. 2(b). However, the periodic case is more complicated because the current at time t is determined by the voltage history from $t-T_C$ to t, which may cover several periods. Hence calculation based on the TDD technique is essential to gain a complete insight to the quantum ac conductance. The simple 1D atomic chain studied here indicates that for both the bias pulse and sinusoidal driving voltages, behavior emerges in $I(t)$ when the amplitude of the time-dependent field is comparable to the bandwidth of the leads.

Generalization of the 1D model to a real three-dimensional (3D) molecular device in the MMM configuration is possible. In the 3D situation, the equilibrium or steady-state Green's function $\tilde{G}^r$ itself becomes a matrix indexed by atomic orbitals of each atom. One needs to replace each scalar element in the $G^r(t_1,t_2)$ matrix by a block matrix with atomic orbital indexes. The matrices in 3D are therefore larger than those of 1D: the total matrix dimension in 3D is the atomic orbital number multiplying the time domain dimension. Within the TDD approach discussed above, the matrix to be inverted is still relatively small compared with the total matrix. Hence, we conclude that the TDD should be equally effective for 3D situations.

V. SUMMARY

In summary, we have developed a numerical approach to handle time-dependent quantum transport beyond the WBL, based on the NEGF formalism presented in Ref. 16. This numerical approach, termed time domain decomposition, is based on directly solving the Dyson's equation in real time. TDD is numerically feasible for transport problems in MMM devices mainly owing to the fact that the time degree of freedom can be truncated in an open system for the $t=-\infty$ limit. The computational cost of the TDD technique can be roughly estimated by the number of time point, N, which is determined by the cutoff T_C [see Eq. (8)] and time interval Δt. For the numerical examples illustrated in Figs. 2 and 3, we have used $N=200$ and $N=50$, respectively. Generally, N of the order of 10^2-10^3 should be sufficient to derive smooth $I(t)$ curves. The computational memory requirement scales with N^2, and the computational time requirement scales with N^4 for the pulsed signal case and with N^3 for the periodic signal case. We have shown that in both pulse and periodic cases, the matrix operations can be further reduced to an inversion of a small triangular matrix plus several matrix multiplications, and the latter can be easily parallelized for distributed computation. This is an exploration to numerically solve nonequilibrium Green's functions in real time domain as opposed to Fourier transformed energy domain. We believe TDD will be useful as it provides a simple but efficient solution to time-dependent transport problems.

ACKNOWLEDGMENTS

We gratefully acknowledge support by the Natural Science and Engineering Research Council (NSERC) of Canada, le Fonds pour la Formation de Chercheurs et l'Aide à la Recherche de la Province du Québec, and NanoQuebec (H.G.). J.W. acknowledges support by a RGC grant from the SAR Government of Hong Kong under Grant No. HKU 7032/03P.

APPENDIX:

In this Appendix, we outline the derivation of the analytical solution to the exactly solvable transport problem discussed in Sec. III. The problem is described as follows: consider a device whose scattering region has of a single energy level, and the device is coupled to a single lead with *finite band width W* (Lorentzian shape). The retarded self-energy of such a lead can be obtained as in Eq. (9). At time $t=0$, the energy level abruptly jumps from E_1 to E_2 due to some external perturbation.

To solve the Green's functions of this problem exactly, we Fourier transform $\Sigma^r(\epsilon)$ of Eq. (9):

$$\Sigma^r(t_1,t_2) = \int \frac{d\epsilon}{2\pi} e^{-i\epsilon(t_1-t_2)} \frac{\Gamma}{2} \frac{W}{\epsilon + iW} = -i\theta(t_1-t_2)\frac{\Gamma}{2} W e^{-W(t_1-t_2)}.$$

The retarded Green's function of the decoupled quantum level (without the lead) can be easily derived as

$$g^r(t_1>0,t_2>0) = -i\theta(t_1-t_2)e^{-iE_1(t_1-t_2)},$$

$$g^r(t_1<0,t_2<0) = -i\theta(t_1-t_2)e^{-iE_2(t_1-t_2)},$$

$$g^r(t_1>0,t_2<0) = -ie^{-i(E_2t_1-E_1t_2)},$$

$$g^r(t_1<0,t_2>0) = 0.$$

The total Green's function of this quantum level coupled with the lead satisfies the integral Dyson equation

$$G^r(t_1,t_2) = g^r(t_1,t_2) + \int\int dt_3 dt_4 g^r(t_1,t_3)\Sigma^r(t_3,t_4)G^r(t_4,t_2).$$

For simplicity, this integral equation can be written in a matrix notation

$$G^r = g^r + g^r\Sigma^r G^r. \tag{A1}$$

The Green's function and the self-energy of Eq. (A1) can be subdivided into a 2×2 block matrix according to $t>0$ and $t<0$, so that the Dyson Eq. (A1) has the form (+ for $t>0$ and − for $t<0$):

$$\begin{pmatrix} G^r_{--} & 0 \\ G^r_{+-} & G^r_{++} \end{pmatrix} = \begin{pmatrix} g^r_{--} & 0 \\ g^r_{+-} & g^r_{++} \end{pmatrix} + \begin{pmatrix} g^r_{--} & 0 \\ g^r_{+-} & g^r_{++} \end{pmatrix} \begin{pmatrix} \Sigma^r_{--} & 0 \\ \Sigma^r_{+-} & \Sigma^r_{++} \end{pmatrix} \times \begin{pmatrix} G^r_{--} & 0 \\ G^r_{+-} & G^r_{++} \end{pmatrix}.$$

This matrix equation can be solved as

$$G^r_{--} = (I - g^r_{--}\Sigma^r_{--})^{-1} g^r_{--},$$

$$G^r_{++} = (I - g^r_{++}\Sigma^r_{++})^{-1} g^r_{++},$$

$$G^r_{+-} = (I + G^r_{++}\Sigma^r_{++}) g^r_{+-} (I + \Sigma^r_{--} G^r_{--}) + G^r_{++}\Sigma^r_{+-} G^r_{--},$$

$$G^r_{-+} = 0. \tag{A2}$$

We emphasize that the right-hand side of expressions (A2) are the matrix form of time integrals. The remaining task is to evaluate them. For G^r_{--} and G^r_{++}, we obtain

$$G^r_{--}(t_1,t_2) = \int \frac{d\epsilon}{2\pi} e^{-i\epsilon(t_1-t_2)} \frac{1}{\epsilon - E_1 - \Sigma^r(\epsilon)},$$

$$G^r_{++}(t_1,t_2) = \int \frac{d\epsilon}{2\pi} e^{-i\epsilon(t_1-t_2)} \frac{1}{\epsilon - E_2 - \Sigma^r(\epsilon)},$$

in which the energy integrals on the right hand side can be easily evaluated by residual summation.

Next, G^r_{+-} has two terms denoted by $G^r_{+-}(I)$ and $G^r_{+-}(II)$, which can be explicitly expressed as

$$G^r_{+-}(I) = \int dt_3 \theta(t_3) \int dt_4 \theta(-t_4) \int \frac{d\epsilon_1}{2\pi} \int \frac{d\epsilon_2}{2\pi} e^{-i\epsilon_1(t_1-t_3)} \times \left[1 + \frac{\Sigma^r(\epsilon_1)}{\epsilon_1 - E_2 - \Sigma^r(\epsilon_1)}\right](-i) e^{-i(E_2 t_3 - E_1 t_4)} e^{-i\epsilon_2(t_4-t_2)} \times \left[1 + \frac{\Sigma^r(\epsilon_2)}{\epsilon_2 - E_1 - \Sigma^r(\epsilon_2)}\right]. \tag{A3}$$

$$G^r_{+-}(II) = \int dt_3 \theta(t_3) \int dt_4 \theta(-t_4) \int \frac{d\epsilon_1}{2\pi} \int \frac{d\epsilon_2}{2\pi} \times e^{-i\epsilon_1(t_1-t_3)} \frac{1}{\epsilon_1 - E_2 - \Sigma^r(\epsilon_1)}(-i) \times \frac{\Gamma}{2} W e^{-W(t_3-t_4)} e^{-i\epsilon_2(t_4-t_2)} \frac{1}{\epsilon_2 - E_1 - \Sigma^r(\epsilon_2)}. \tag{A4}$$

Using the identity

$$\int dt \theta(\pm t) e^{i\epsilon t} = \frac{i}{\pm\epsilon + i0^+},$$

one can evaluate the time integrals and energy integrals in expressions (A3) and (A4). The results are given in Eqs. (10)–(13).

Finally, the time-dependent current can be expressed in terms of the Green's functions as

$$I(t) = \theta(t) 2\,\mathrm{Re}\left[G^r_{++}\Sigma^<_{++} + G^r_{+-}\Sigma^<_{-+} + G^<_{++}\Sigma^a_{++} + G^<_{+-}\Sigma^a_{-+}\right]_{tt},$$

where

$$G^<_{+-} = G^r_{++}\Sigma^<_{+-}G^a_{--} + G^r_{+-}\Sigma^<_{--}G^a_{--},$$

$$G^<_{++} = G^r_{++}\Sigma^<_{++}G^a_{++} + G^r_{+-}\Sigma^<_{-+}G^a_{++} + G^r_{++}\Sigma^<_{+-}G^a_{-+} + G^r_{+-}\Sigma^<_{--}G^a_{-+}.$$

Notice that all the time dependence in G^r are in the exponential form. After further tedious but straightforward algebra, these time integrals in the last two equations can be evaluated analytically, and the current $I(t)$ can be written in the form of a single integral over energy (not shown). We then use this exactly solved $I(t)$ to compare with the numerical results obtained by TDD. Because the results are indistinguishable, in Fig. 1 only the curve from TDD is shown.

[1] A. Aviram and M. Ratner, Chem. Phys. Lett. **29**, 277 (1974).

[2] For a recent review on molecular electronics, see for example, A. Nitzan and M. A. Ratner, Science **300**, 1384 (2003).

[3] M. A. Reed, C. Zhou, C. J. Muller, T. P. Burgin, and J. M. Tour, Science **278**, 252 (1997); D. J. Wold, R. Haag, M. A. Rampi, and C. D. Frisbie, J. Phys. Chem. B **106**, 2813 (2002); T. Ishida, W. Mizutani, Y. Aya, H. Ogiso, S. Sasaki, and H. Tokumoto, *ibid.* **106**, 5886 (2002).

[4] D. J. Wold and C. D. Frisbie, J. Am. Chem. Soc. **122**, 2970 (2000); X. D. Cui, A. Primak, X. Zarate, J. Tomfohr, O. F. Sankey, A. L. Moore, T. A. Moore, D. Gust, G. Harris, and S. M. Lindsay, Science **294**, 571 (2001); D. J. Wold and C. D. Frisbie, J. Am. Chem. Soc. **123**, 5549 (2001); J. Zhao and K. Uosaki, Nano Lett. **2**, 137 (2002); J. M. Beebe, V. B. Engelkes, L. L. Miller, and C. D. Frisbie, J. Am. Chem. Soc. **124**, 11268 (2002); B. Xu and N. J. Tao, Science **301**, 1221 (2003); T. Lee, W. Wang, J. F. Klemic, J. J. Zhang, J. Su, and M. A. Reed, J. Phys. Chem. B **108**, 8742 (2004).

[5] R. M. Metzger, Acc. Chem. Res. **32**, 950 (1999); J. Reichert, R. Ochs, D. Beckmann, H. B. Weber, M. Mayor, and H. v. Löhneysen, Phys. Rev. Lett. **88**, 176804 (2002); C. Kergueris, J.-P. Bourgoin, S. Palacin, D. Esteve, C. Urbina, M. Magoga, and C. Joachim, Phys. Rev. B **59**, 12 505 (1999).

[6] For a recent review on conduction through DNA, see for example, R. G. Endres, D. L. Cox, and R. R. P. Singh, Rev. Mod. Phys. **76**, 195 (2004).

[7] P. J. Burke, IEEE Trans. Nanotechnol. **2**, 55 (2003).

[8] S. Li, Z. Yu, S.-F. Yen, W. C. Tang, and P. J. Burke, Nano Lett. **4**, 753 (2004).

[9] M. Büttiker, A. Prêtre, and H. Thomas, Phys. Rev. Lett. **70**, 4114 (1993).

[10] B. Wang, J. Wang, and H. Guo, Phys. Rev. Lett. **82**, 398 (1999).

[11] J. Taylor, H. Guo, and J. Wang, Phys. Rev. B **63**, 245407 (2001); **63**, 121104(R) (2001).

[12] M. Brandbyge, J.-L. Mozos, P. Ordejón, J. Taylor, and K. Stokbro, Phys. Rev. B **65**, 165401 (2002).

[13] S.-H. Ke, H. U. Baranger, and W. Yang, Phys. Rev. B **70**, 085410 (2004).

[14] C.-C. Kaun, B. Larade, and H. Guo, Phys. Rev. B **67**, 121411(R) (2003); C. C. Kaun and H. Guo, Nano Lett. **3**, 1521 (2003).

[15] S. K. Nielsen, M. Brandbyge, K. Hansen, K. Stokbro, J. M. van Ruitenbeek, and F. Besenbacher, Phys. Rev. Lett. **89**,

066804 (2002).
[16] A.-P. Jauho, N. S. Wingreen, and Y. Meir, Phys. Rev. B **50**, 5528 (1994).
[17] N. S. Wingreen, A.-P. Jauho, and Y. Meir, Phys. Rev. B **48**, 8487 (1993).
[18] G. P Lopinski, D. D. M. Wayner, and R. A. Wolkow, Nature (London) **406**, 48 (2000); P. Kruse and R. A. Wolkow, Appl. Phys. Lett. **81**, 4422 (2002); X. Tong, G. A. DiLabio, O. J. Clarkin, and R. A. Wolkow, Nano Lett. **4**, 357 (2004).
[19] R. Basu, N. P. Guisinger, M. E. Greene, and M. C. Hersam, Appl. Phys. Lett. **85**, 2619 (2004).
[20] Q. F. Sun, B. G. Wang, J. Wang, and T. H. Lin, Phys. Rev. B **61**, 4754 (2000).
[21] M. Plihal, D. C. Langreth, and P. Nordlander, Phys. Rev. B **61**, R13 341 (2000).
[22] Z. Ma, J. Shi, and X. C. Xie, Phys. Rev. B **62**, 15 352 (2000).
[23] R. López, R. Aguado, G. Platero, and C. Tejedor, Phys. Rev. B **64**, 075319 (2001).
[24] J. C. Cuevas, A. Martín-Rodero, and A. L. Yeyati, Phys. Rev. B **54**, 7366 (1996).
[25] Q.-F. Sun, J. Wang, and T.-H. Lin, Phys. Rev. B **59**, 13 126 (1999).
[26] W. Zheng, Y. Wei, J. Wang, and H. Guo, Phys. Rev. B **61**, 13 121 (2000).
[27] C. Roland, M. B. Nardelli, J. Wang, and H. Guo, Phys. Rev. Lett. **84**, 2921 (2000).
[28] I. Appelbaum, T. Wang, J. D. Joannopoulos, and V. Narayanamurti, Phys. Rev. B **69**, 165301 (2004).